

Analogue modelling of asymmetrical back-arc extension

Wouter P. Schellart

Epsilon Laboratory
Australian Crustal Research Centre
School of Geosciences, P.O. Box 28E, Monash University
Melbourne, VIC 3800, Australia

Gordon S. Lister

Australian Crustal Research Centre
Monash University
Melbourne, VIC 3800, Australia

M. W. Jessell

Epsilon Laboratory
Australian Crustal Research Centre
School of Geosciences, P.O. Box 28E, Monash University
Melbourne, VIC 3800, Australia

Keywords: asymmetry, back-arc basin, modelling, simulation, analogue experiment, subduction, roll-back

Abstract: Back-arc extension takes place in the overriding plate in an overall convergent setting during retreat of the hinge-line of the subducting slab. A large number of back-arc basins display a geometry and internal structure that is asymmetric, i.e. where the amount of extension increases from one end of the arc to the other. We present the results of 3-dimensional analogue modelling of asymmetric back-arc extension of an overriding lithosphere with a varying initial rheology. The results show that with increasing lithospheric brittle to viscous strength (BS/VS), the fault density decreases in magnitude, while the asymmetry in deformation pattern in the back-arc region increases. The area extent of deformation is mainly dependent on the ratio of brittle strength to buoyancy force (BS/BF), i.e. the larger the ratio, the smaller the area of deformation. The experimental results have been compared with several arc - back-arc systems, which display a relatively large amount of structural asymmetry (Tonga Arc, Kuril Arc, New Hebrides Arc, Ryukyu arc) but a varying style of tectonic deformation. These differences are mainly the result of the stage of opening up of the back-arc basin, the subduction setting (ocean-ocean or ocean-continent) and difference in rheology of the overriding lithosphere.

Table of Contents

Introduction	4
Analogue model	5
Results	7
General results	7
Individual experiments	10
Discussion	14
General discussion	14
Discussion (continued)	16
Natural examples of asymmetrical back-arc extension	16
Conclusions	19
References	20

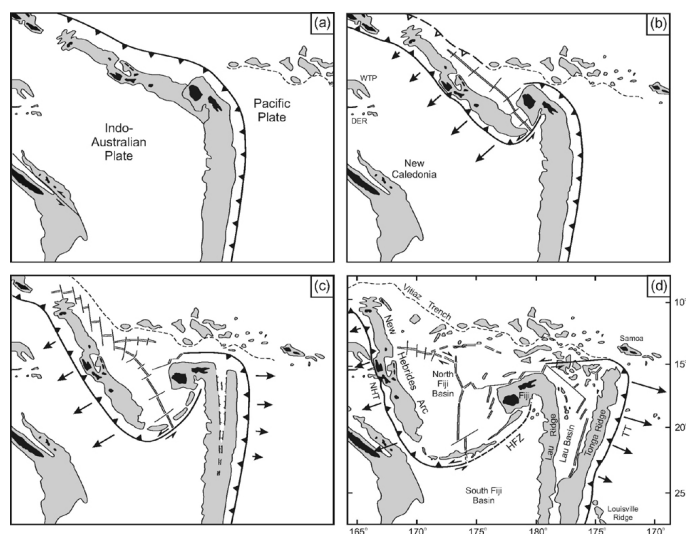
Introduction

Back-arc basins are enigmatic geological features, which form in the overriding plate in overall convergent plate tectonic settings on the concave side of the arc. Back-arc basins occur in two different tectonic regimes: ocean-ocean subduction and ocean-continent subduction. In the former regime, the back-arc basin is commonly found in between a remnant volcanic arc and the active volcanic arc, which were separated during back-arc opening. In ocean-ocean subduction settings extension is often localised along narrow rift segments or along clear defined spreading ridges. Some examples include the Mariana Arc, the Izu-Bonin Arc, the Tonga Arc, the Kermadec Arc, the New Hebrides Arc, the Scotia Arc and the Lesser Antilles Arc. In the latter regime, the back-arc basin is located on the continental lithosphere. This often results in more diffuse extension over a large area. Examples include the Kuril Arc, the Japan Arc, the Ryukyu Arc, the Banda Arc, the Hellenic Arc, the Calabrian Arc, the Betic-Rif Arc and the Carpathian Arc.

Back-arc extension involves regressive (oceanward) hinge-line (or trench axis) migration of the subducting plate (i.e. rollback). Whether this regressive movement is the cause or the effect of back-arc extension remains a debate, but presently the majority of geoscientists favour the former view. In this sense, rollback is driven by the negative buoyancy of the subducting slab compared to the asthenosphere [Elsasser 1971; Molnar and Atwater 1978]. Hence, rollback provides space along the plate boundary. This space is filled by the overriding plate, which passively follows the retreating hinge of the subducting slab.

Slab rollback is primarily driven by its negative buoyancy compared to the asthenosphere, which is often related to age of the oceanic lithosphere (i.e. the older, the colder, the denser). However, the actual retreat velocity depends on a variety of factors, including negative buoyancy of the slab, tearability of the slab, ability of asthenosphere material underneath the slab to migrate towards the slab corner and viscosity of the asthenosphere.

Figure 1. Tectonic reconstruction of the New Hebrides - Tonga region - Tonga region

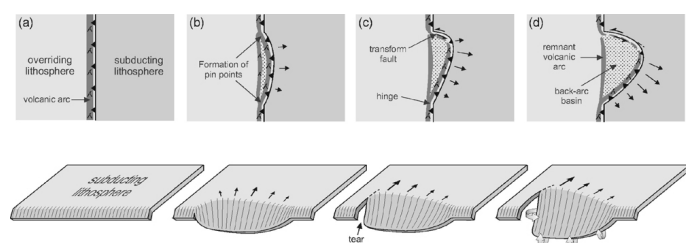


Tectonic reconstruction of the New Hebrides - Tonga region (modified and interpreted from Auzende *et al.* [1988], Pelletier *et al.* [1993], Hathway [1993] and Schellart *et al.* [2002a]) at (a) ~ 13 Ma, (b) ~ 9 Ma, (c) 5 Ma and (d) Present. The Indo-Australian plate is fixed. DER = d'Entrecasteaux Ridge, HFZ = Hunter Fracture Zone, NHT = New Hebrides Trench, TT = Tonga Trench, WTP = West Torres Plateau. Arrows indicate direction of arc migration. During opening of the North Fiji Basin, the New Hebrides block has rotated some 40-50° clockwise [Musgrave and Firth 1999], while the Fiji Plateau has rotated some 70-115° anticlockwise [Malahoff *et al.* 1982]. During opening of the Lau Basin, the Tonga Ridge has rotated ~ 20° clockwise [Sager *et al.* 1994]. (Click for enlargement)

From geological, structural, geomorphological, magnetic lineation and paleomagnetic data it is clear that different arc - back-arc systems evolve quite differently (Schellart *et al.* 2002b). For instance, several arcs seem to have formed by radial spreading, resulting in symmetrical arc development with arc-parallel and arc-perpendicular extension in the overriding plate and equal amounts of block rotation on each side of the arc. Examples could be the Hellenic Arc and Aegean Sea, the Ryukyu Arc and Okinawa Trough, and the Carpathian Arc and Pannonian Basin. Another group of arcs seems to have developed due to asymmetrical spreading. Two examples for this type of spreading are the New Hebrides Arc (Schellart *et al.* 2002a) and the Tonga Arc, located in the southwest Pacific (Figure 1). For each of these two arcs, its back-arc basin has opened up in a wedge shaped manner, with an increasing opening rate from one side of the arc to the other. Development of

such arc systems involves asymmetrical back-arc spreading with similar magnitude and sense of rotation along the arc and shearing (with possible related block rotations) at the side of the arc (Figure 2). Other examples of this arc configuration could include the Kuril Arc and Sea of Okhotsk + Kuril Basin, the Japan Arc and Japan Sea, the Calabria – Apennines Arc and Thyrrenian Sea, and rotation of the Corsica-Sardinia block and opening of the Ligurian Sea. Also, the late stage development of both the Hellenic Arc and the Ryukyu Arc could have resulted from asymmetrical spreading.

Figure 2. Development of asymmetrical arcs during asymmetrical rollback



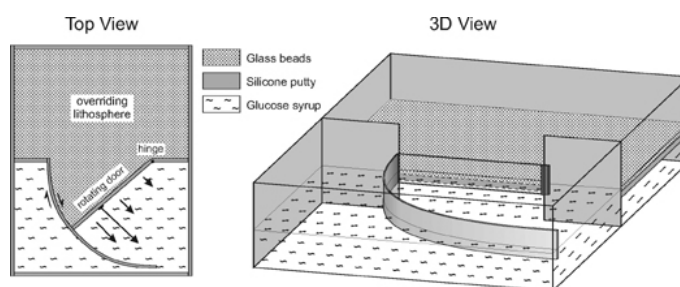
Schematic sketches of development of asymmetrical arc during asymmetrical rollback of subducting slab in plan view (top) and 3D view (bottom). (a) Initial state with rectilinear subduction zone; (b) initiation of rollback with formation of pin points or cusps (points where subducting slab is resisting to roll back); (c) one pin point evolves into transform plate boundary due to formation of vertical tear in subducting slab, while other becomes a hinge point along which the arc rotates; (d) progressive growth of tear and continued rotation around hinge point. Black arrows indicate direction of hinge-line migration. Thick arrows in (d) indicate direction of asthenosphere flow to accommodate slab retreat.

In this paper we will focus on arc - back-arc systems which form by asymmetrical spreading. We will investigate this type of asymmetrical deformation by means of small-scale analogue experiments. In these experiments the model apparatus configuration remains unaltered, but the rheology of the overriding plate is varied systematically for different experiments. We will compare these results briefly with some natural examples of arc - back-arc systems, which display structural features, which could testify to a development resulting from asymmetrical spreading. Finally, the results of these experiments will be discussed and placed in a tectonic context of rollback as a driving mechanism for large-scale extensional features, including Cenozoic extension along the East Asian margin.

Analogue model

The scaling theory for analogue modelling of geologic processes has first been described by Hubbert [1937] and has later also been discussed by Horsfield [1977], Davy and Cobbold [1991] and Cobbold and Jackson [1992]. Here, the most important relationship is the one that relates surface forces (stresses) to body forces (gravity). When the experiments are executed in a normal field of gravity, stresses should be scaled down as the product of density and length scales down [Horsfield 1977; Davy and Cobbold 1991]. In the experiments described here a scale factor of $\sim 1-2.5 \times 10^{-7}$ (1 cm in experiment resembles $\sim 40-100$ km in nature) and a density factor of ~ 0.5 have been applied, thus stresses should be scaled down by $\sim 1.25 \times 10^{-7} - 5 \times 10^{-8}$. For brittle rocks, their cohesion and friction coefficient are the most important parameters, as described by Coulomb's fracture criterion [Coulomb, 1776]. Since cohesion has the dimensions of Pascal (Pa), it should be scaled down in a similar fashion as stresses [Davy and Cobbold 1991; Cobbold and Jackson 1992]. Furthermore, the friction coefficient is dimensionless, thus it should have similar values in both model and nature. Finally, for viscous material, viscosity should scale down as the product of stresses and time scales down [Davy and Cobbold 1991]. The experiments described here are executed in the normal field of gravity and the materials used in the experiments have been chosen as such, that they have been properly scaled to model the deformation of natural rocks.

Figure 3. Schematic sketch of experimental apparatus



Schematic sketch of experimental apparatus used to investigate asymmetrical back-arc spreading of a two-layered brittle-ductile plate, simulating the overriding lithosphere, during asymmetrical opening of a door, simulating the asymmetric hinge-line retreat of the subducting lithosphere. The model lithosphere is underlain by glucose syrup, simulating the asthenosphere, which gives the lithosphere isostatic support.

A model has been constructed to simulate back-arc extension in the overriding plate due to asymmetrical roll-back. The model consists of only three layers in order to preserve the simplicity of the experiment (e.g. conform Hatzfeld *et al.* [1997], Gautier *et al.* [1999] and Martinod *et al.* [2000]). The layered system is confined in a 60 by 40 cm box. On one side of the box a rotational sidewall is situated, which can rotate outwards in an anticlockwise fashion (Figure 3), simulating the progressive anticlockwise retreat of the hinge-line of the subducting plate. The uppermost two layers represent the overriding lithosphere. The lowermost layer represents the asthenosphere and gives the overlying lithosphere isostatic support. The uppermost brittle layer is made of fine-grained glass microspheres simulating the brittle upper lithosphere in nature,

which are properly scaled to model brittle behaviour of rocks, especially when used for extension related experiments [Schellart 2000]. The high viscosity middle layer is made of silicone putty (mixed with a dense filler) with a viscosity of $\sim 2 \times 10^4$ Pa·s, simulating the viscous lower lithosphere in nature. The lowermost viscous layer is made of glucose syrup with a viscosity of ~ 100 Pa·s. The experimental properties of the individual experiments discussed in the text are given in Table 1. The progressive opening of the sidewall is driven by a step-motor. A passive grid (line spacing = 3 cm) and marker spheres have been laid on top of the brittle layer to monitor displacement and deformation. The progressive development of the model has been recorded by a digital camera from above, under oblique lighting of the top surface of the experiment.

Table 1. Experimental properties

Experiment	Material	Rheology	Layer Thickness (cm)	Opening rate (°/hr)	Density
1	Microspheres	Brittle	0.4	21	1.22
	Silicone	High-viscosity	1.2		1.22
	Glucose	Low-viscosity	5.5		1.42
2	Microspheres	Brittle	0.4	12	1.22
	Silicone	High-viscosity	1.2		1.22
	Glucose	Low-viscosity	5.5		1.42
3	Microspheres	Brittle	0.6	12	1.22
	Silicone	High-viscosity	1.2		1.22
	Glucose	Low-viscosity	5.5		1.42
4	Microspheres	Brittle	0.6	12	1.22
	Silicone+sand	Viscoplastic	0.2		1.22
	Silicone	High-viscosity	1.0		1.22
	Glucose	Low-viscosity	5.5		1.42
5	Microspheres	Brittle	0.6	36	1.22
	Silicone	High-viscosity	0		-
	Glucose	Low-viscosity	5.5		1.42
6	Microspheres	Brittle	0.5	12	1.22
	Silicone	High-viscosity	1.2		1.22
	Glucose	Low-viscosity	5.5		1.42
7	Microspheres	Brittle	.6	12	1.22
	Silicone	High-viscosity	0		-
	Glucose	Low-viscosity	5.5		1.42
8	Microspheres	Brittle	0.5	4	1.22
	Silicone	High-viscosity	1.2		1.22
	Glucose	Low-viscosity	5.5		1.42
9	Microspheres	Brittle	0.8	21	1.32
	Silicon	High-viscosity	1.0		1.32
	Glucose	Low-viscosity	5.5		1.42

Results

General results

Experiments with different ratios of brittle to viscous layer thickness (and therefore strength) have been executed. The results demonstrate that with increasing brittle strength to viscous strength ratio (BS/VS), deformation becomes more localised with fewer faults absorbing more deformation. In other words, the fault density decreases with increasing BS/VS ratio. This can be observed in Figure 4, where the resulting strain patterns and interpretations

of 9 experiments have been plotted (some of the physical properties for the experiments are given in Table I and 2). Furthermore, the surface extent of deformation inside the box decreases with increasing brittle strength to buoyancy force ratio (BS/BF) (Figure 5). For all the experiments, the extent of the deformed area rapidly increases in magnitude in the first 10-30° of rotation and then slows down until it stagnates (except for experiment 1) (Figure 5). For relatively high BS/VS ratios, the rapid increase takes place in the first ~ 10° (experiments 5, 7 and 8), while for relatively

low BS/VS ratios, this occurs in the first $\sim 30^\circ$ (experiments 1, 2, 3, 6 and 9).

Figure 4a, 4b, and 4c. Photographs and interpretation of experiments

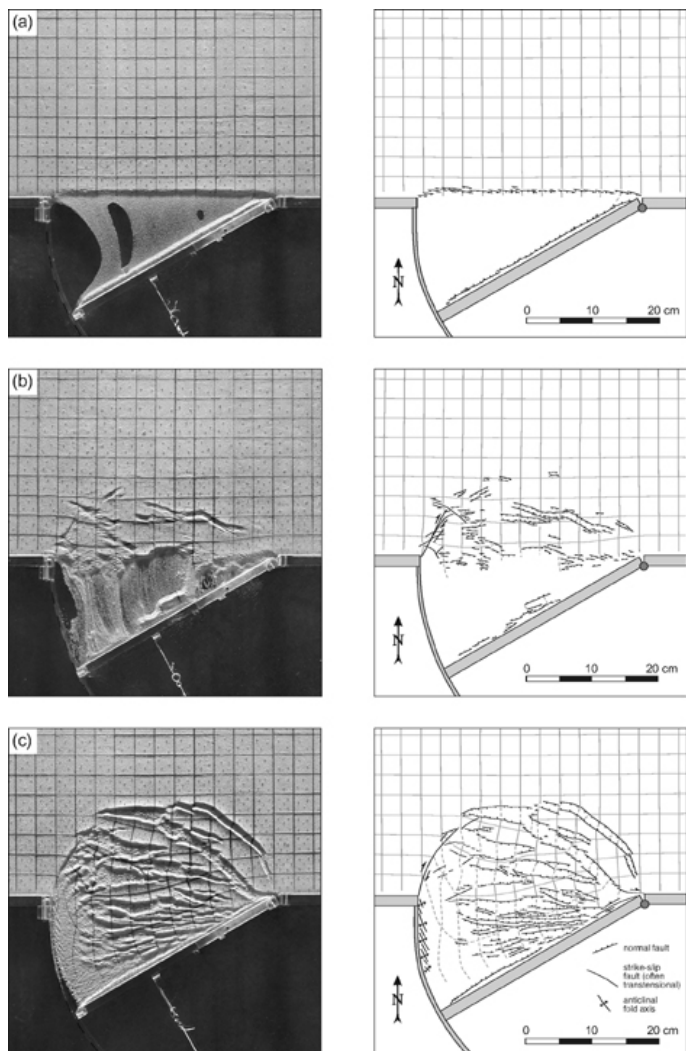
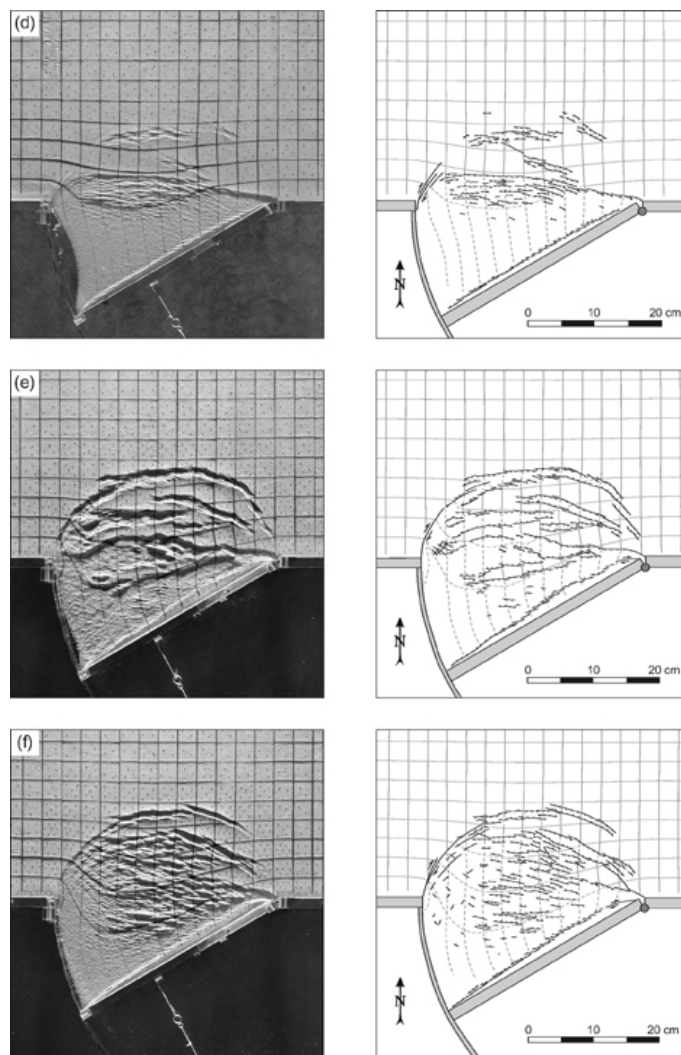


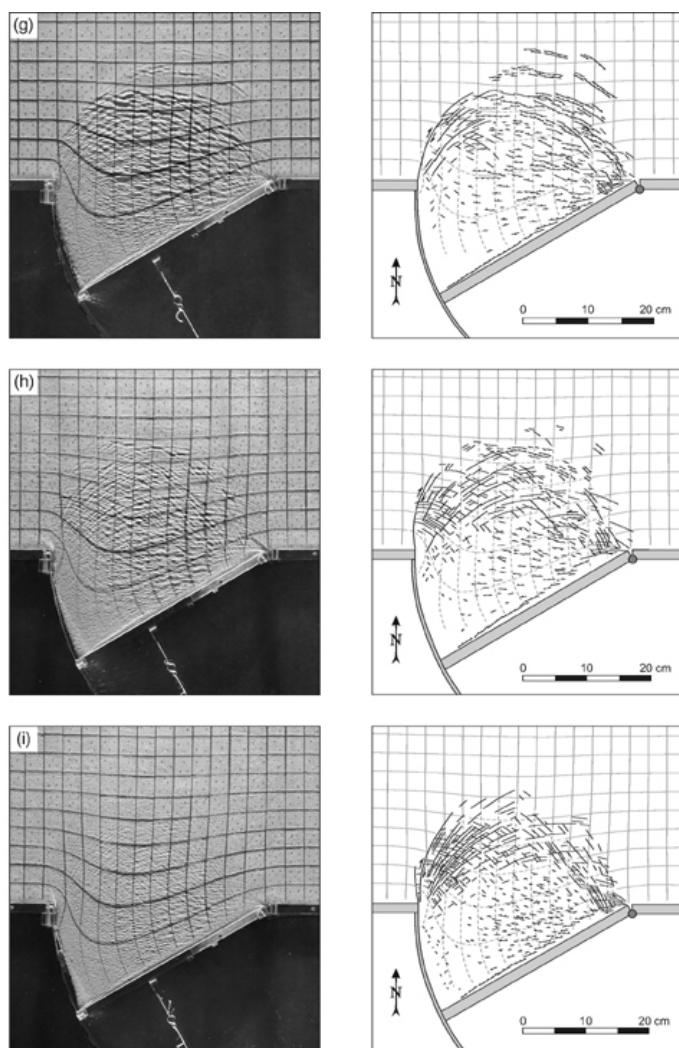
Figure 4d, 4e and 4f. (continued)



(d) BS/VS ~ 16 (exp. 9) (e) BS/VS ~ 12.5 (exp.4) and (f) BS/VS ~ 8.3 (exp. 3).

Photographs (left) and interpretation (right) of experiments with different styles of extension for different ratios of brittle strength versus viscous strength (BS/VS) and different buoyancy force of the lithosphere. (a) BS/VS > 25 (exp. 7), (b) BS/VS ~ 25 (exp. 5), (c) BS/VS ~ 18 (exp. 8). All of the images are after 30° of rotation.

Figure 4g, 4h and 4i. (continued)



(g) BS/VS ~ 6, (exp. 6), (h) BS/VS ~ 4 (exp. 2) and (i) BS/VS ~ 2.4 (exp. 1).

Table 2. Experimental ratios for different experiments

Experiment	Layer thickness ratio (B/V)	BS/VS (N/m / N/m)	Buoyancy Force (N/m)	BS/BF	IS/BF
1	0.4/1.2	0.12/0.05	0.21	0.57	0.81
2	0.4/1.2	0.12/0.03	0.21	0.57	0.71
3	0.6/1.2	0.25/0.03	0.27	0.93	1.04
4	0.6/1.0	~0.25/ ~0.02	0.27	0.93	1.00
5	0.6/0.0	0.25/ ~0.01	0.03	8.33	8.67
6	0.5/1.2	0.18/0.03	0.24	0.75	0.88
7	0.6/0.0	0.25/ ~0.00	0.03	8.33	8.33
8	0.5/1.2	0.18/0.01	0.214	0.75	0.79
9	0.8/1.0	0.48/0.03	0.09	5.33	5.67

Note

B = brittle, V = viscous, BS = brittle integrated strength, VS = viscous integrated strength, IS = total integrated strength, BF = buoyancy force.

For an opening rate of 12°/h the average strain rate was estimated at ~ 10⁻⁴ s⁻¹. It should be noted that the strain rate is highly variable in an experiment, due to the asymmetrical opening in the experiment as well as the decrease in strain rate away from the retreating boundary.

For the two-layer lithosphere experiments (experiments 1-4, 6, 8 and 9), the asymmetry in the deformation pattern is more pronounced in the northern part of the deformed zone with increasing BS/VS ratio. Here, most deformation is accommodated by normal faults, which increase in strike

angle relative to the retreating door towards the north and east (Figure 4c-f). In contrast, with a relatively low BS/VS ratio, deformation in the north is absorbed by conjugate strike-slip faults (with a component of transtension) (Figure 4h,i). All of the experiments (except experiment 5) showed the formation of a relatively undeformed continuous strip of lithosphere along the boundary of the retreating door, behind which extension was greatest.

Figure 5. Diagram showing the increase in deformed area

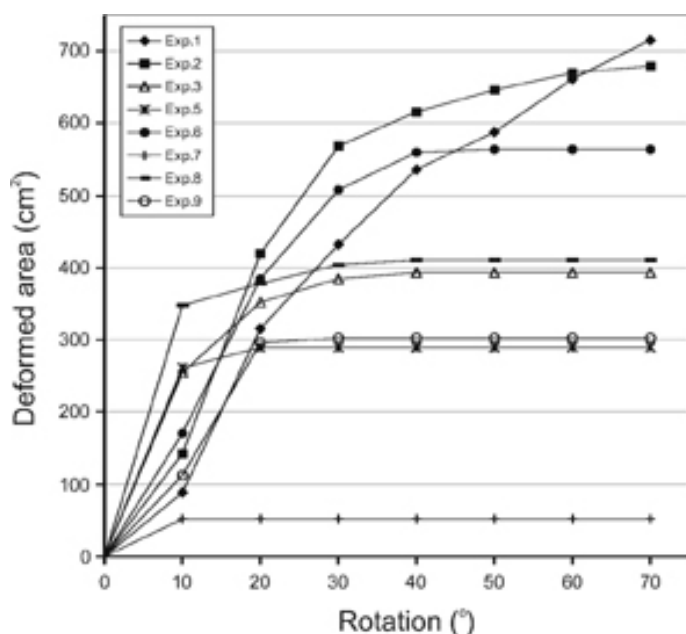


Diagram showing the increase in deformed area inside the box (i.e. north of the gate) for every 10° increment of rotation of the door for different experiments.

For experiments in which rift systems were well developed, these rift structures displayed rift shoulder uplift, resulting from the isostatic support of the lithosphere provided by the underlying glucose syrup.

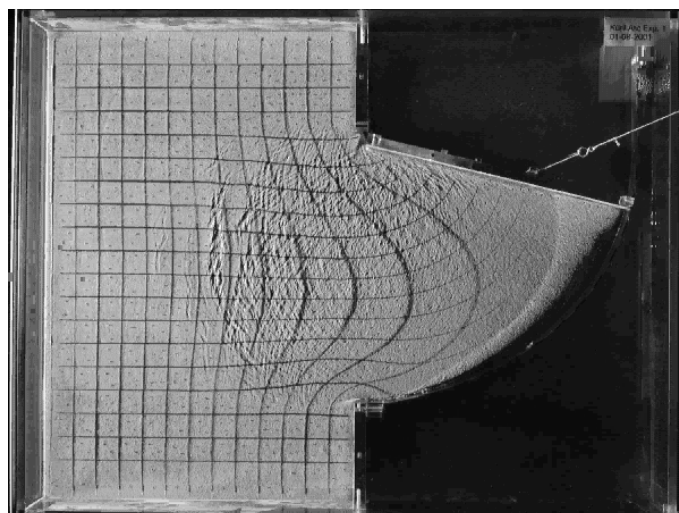
Individual experiments

In this section the results of experiments 1 to 9 will be described individually (see Figure 4 and movies).

Experiment 7 (Figure 4a, movie 1): In this experiment, the brittle top layer (0.6 cm) was directly superposed on top of the glucose syrup. This resulted in a very localised deformation pattern close to the gate, which got established within the first ~ 5° of rotation. Faulting was restricted to a rift system striking parallel to the door with normal faults striking slightly oblique to the rift axis. However, slight

amounts of stretching of the brittle layer north of the rift zone was evident from the curvature of the east-west oriented grid lines. In between the rift system and the retreating door a narrow ridge developed.

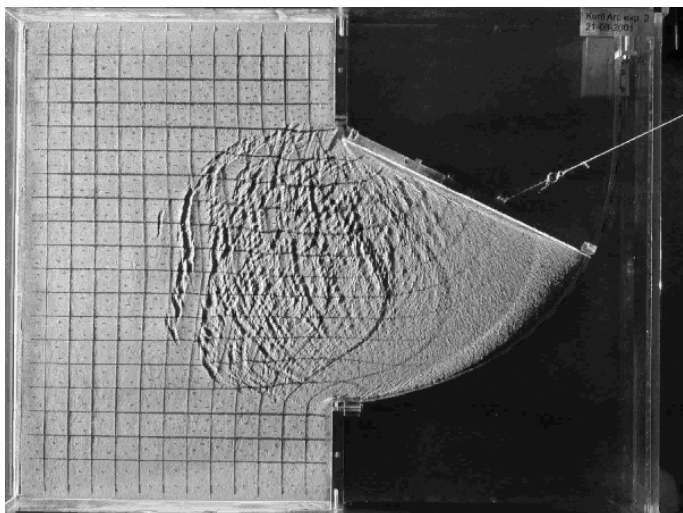
Figure 1. Experiment 7



The brittle top layer (0.6 cm) was directly superposed on top of the glucose syrup.

Experiment 5 (Figure 4b, movie 2): In this experiment, the brittle top layer (0.6 cm) was directly superposed on top of the glucose syrup and the rate of opening was three times faster than in experiment 7. This resulted in a very localised and irregular deformation pattern, which rapidly migrated towards the north within the first ~ 10° of rotation but then stopped migrating and formed a through-going irregular rift structure parallel and closely behind the retreating door. This structure absorbed all of the continued extension. Most deformation in this experiment was accommodated by normal faults. A small number of strike-slip faults developed near the western corner of the gate.

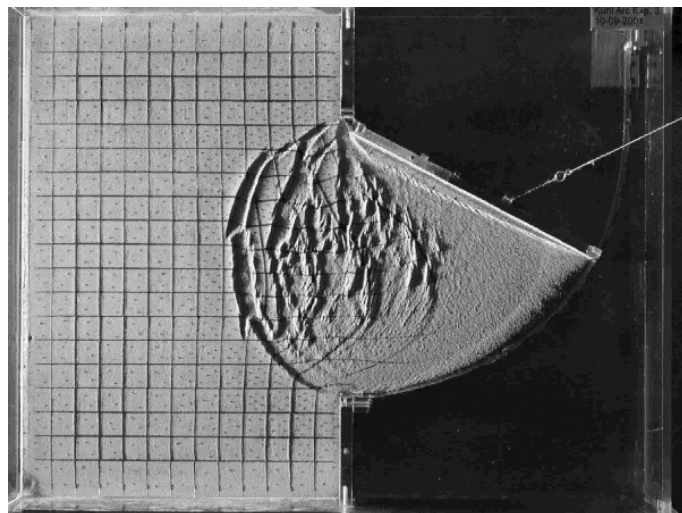
Figure 2. Experiment 5



In this experiment, the brittle top layer (0.6 cm) was directly superposed on top of the glucose syrup and the rate of opening was three times faster than in experiment 7.

Experiment 8 (Figure 4c, movie 3): In this experiment, the brittle layer (0.5 cm) was superposed on the silicone layer (1.2 cm), overlying the glucose syrup, and the opening rate of the door was relatively slow ($4^\circ/\text{h}$). This resulted in a relatively localised strain pattern, although less irregular compared to experiment 5. The deformation front migrated towards the north within the first $\sim 15^\circ$ of rotation and then stopped migrating. From this time onwards, the extension was limited to the deformed zone. In between the extending zone and the retreating door a relatively undeformed thin strip of material developed. In this experiment most deformation was absorbed by normal faults, while a few strike-slip faults developed along the western side of the deformed zone striking north to northeast. The normal faults obtained a strike oriented E-W in the west but progressively more NNW-SSE towards the east.

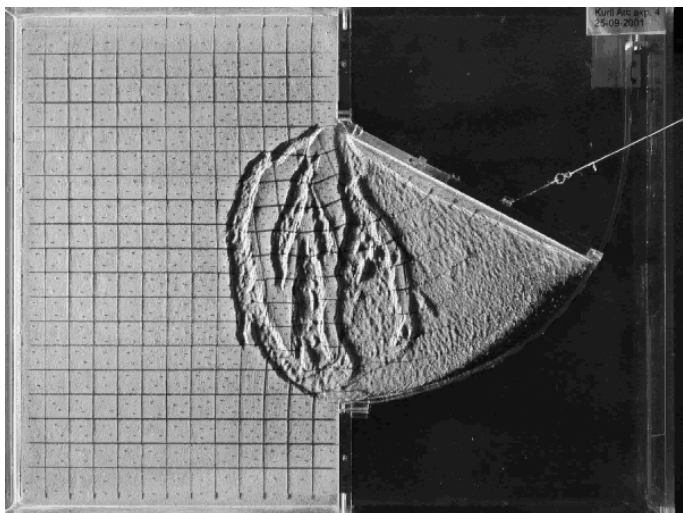
Figure 3. Experiment 8



the brittle layer was superposed on the silicone layer overlying the glucose syrup, and the opening rate of the door was relatively slow.

Experiment 9 (Figure 4d, movie 4): In this experiment, the brittle layer (0.8 cm) was superposed on the silicone layer (1.0 cm), overlying the glucose syrup. Again, this resulted in a relatively localised strain pattern. The deformation front rapidly migrated towards the north within the first 20° of rotation and then stopped migrating. From this time onwards, the extension was localised along a through going extending zone located just north of the retreating boundary, with in between a relatively undeformed strip of material. In this experiment most deformation was absorbed by normal faults, while a small number of strike-slip faults developed near the western corner of the gate striking northeast to north-northeast. The normal faults obtained a strike oriented E-W in the west but progressively more WNW-ESE towards the east.

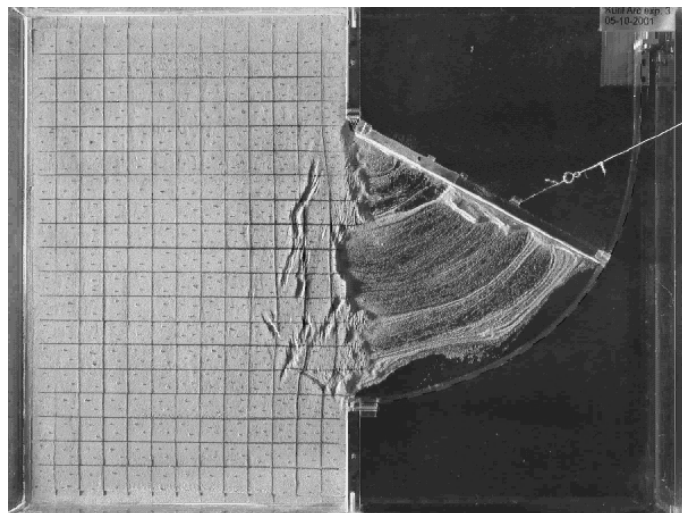
Figure 4. Experiment 9



The brittle layer was superposed on the silicone layer overlying the glucose syrup.

Experiment 4 (Figure 4e, movie 5): In this experiment, a viscoplastic layer (0.2 cm) was inserted in between the brittle layer (0.6 cm) and the viscous layer (1.0 cm). This resulted in a localised deformation with well-defined elongated rift structures bounding relatively undeformed microplate-like segments. The deformation front migrated towards the north up to $\sim 20^\circ$ of rotation. Soon after, extension was mainly focussed along a through going extending zone located just north of the retreating boundary. As in most other experiments, a relatively undeformed strip of material developed in between the extending zone and the retreating door. Most deformation was absorbed by normal faults, while a small number of dextral strike-slip faults developed near the western corner of the gate striking northeast to north-northeast. The normal faults obtained a strike oriented E-W in the west, which became oriented progressively more NNW-SSE towards the east.

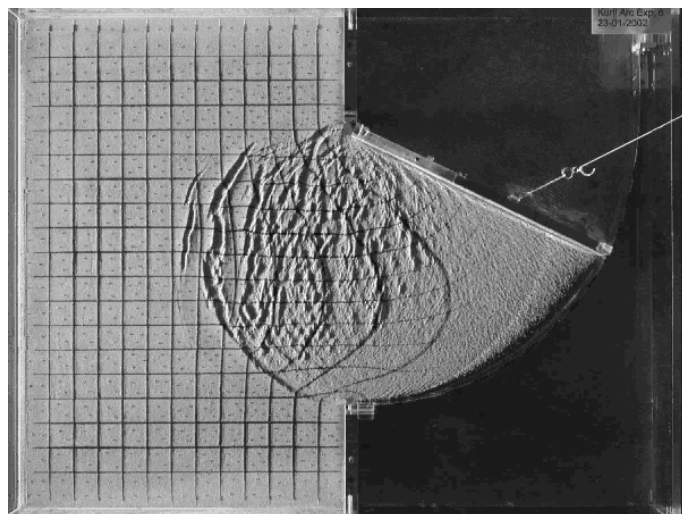
Figure 5. Experiment 4



A viscoplastic layer was inserted in between the brittle layer and the viscous layer (1.0 cm).

Experiment 3 (Figure 4f, movie 6): Here, a brittle (0.6 cm) layer was superposed on top of a viscous layer (1.2 cm), overlying glucose syrup. This resulted in a deformation pattern similar to that of experiment 4, although it is more diffuse with less well defined graben structures close to the retreating boundary. The deformation front migrated towards the north up to $\sim 25^\circ$ of rotation. Extension continued in the entire deformed region, but the amount of extension absorbed by the region close to the retreating boundary increased.

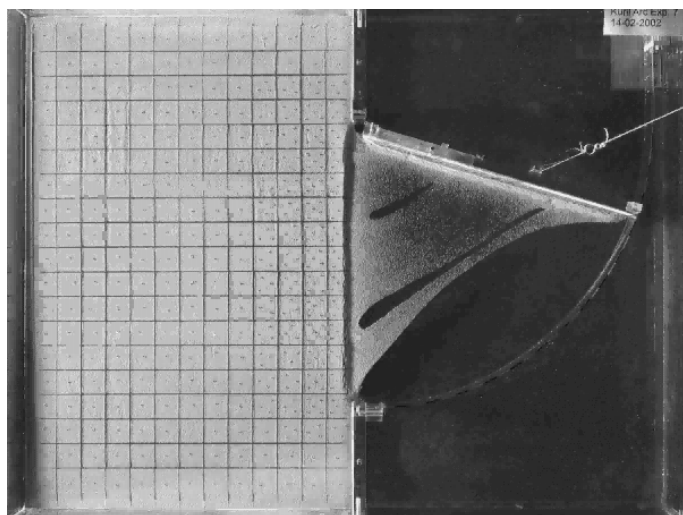
Figure 6. Experiment 3



A brittle (0.6 cm) layer was superposed on top of a viscous layer (1.2 cm), overlying glucose syrup.

Experiment 6 (Figure 4g, movie 7): In this experiment, a brittle (0.5 cm) layer was superposed on top of a viscous layer (1.2 cm), overlying glucose syrup. This resulted in a more diffuse deformation pattern compared to experiment 3. The deformation front migrated towards the north up to $\sim 35^\circ$ of rotation. Extension continued in the entire deformed region, but the amount of extension absorbed by the region close to the retreating boundary increased. As in most experiments, a relatively undeformed strip of material developed in between the extending zone and the retreating door. Close to the retreating boundary normal faulting was the dominant type of deformation, while near the corners and further to the north deformation was mainly absorbed by conjugate (transtensional) strike-slip faults.

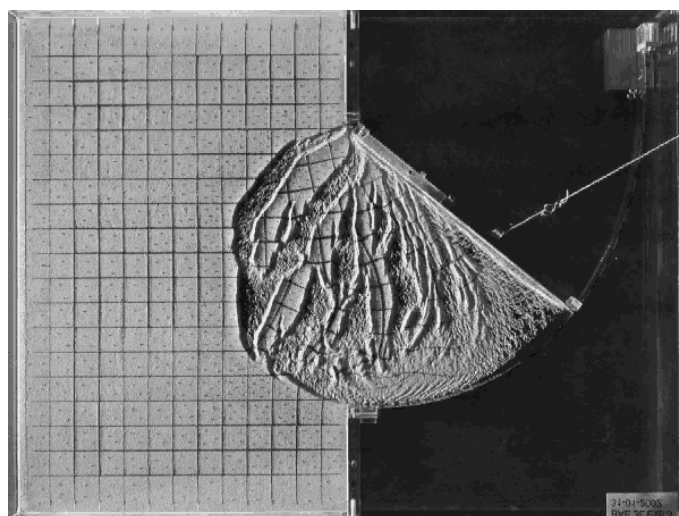
Figure 7. Experiment 6



A brittle layer was superposed on top of a viscous layer overlying glucose syrup.

Experiment 2 (Figure 4h, movie 8): In this experiment, a brittle (0.4 cm) layer was superposed on top of a viscous layer (1.2 cm), overlying glucose syrup. This resulted in a diffuse deformation pattern. The deformation front migrated towards the north up to $\sim 55^\circ$ of rotation. Extension continued in the entire deformed region, but the amount of extension absorbed by the region close to the retreating boundary increased. Again, a relatively undeformed strip of material developed in between the extending zone and the retreating door. Close to the retreating boundary normal faulting is the dominant type of deformation, while near the corners and further to the north deformation is mainly absorbed by conjugate (transtensional) strike-slip faults.

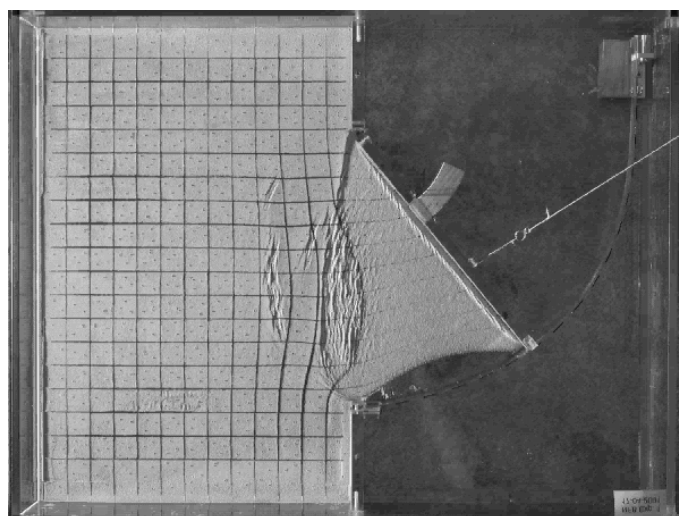
Figure 8. Experiment 2



A brittle layer was superposed on top of a viscous layer overlying glucose syrup.

Experiment 1 (Figure 4i, movie 9): In experiment 1, a brittle (0.4 cm) layer was superposed on top of a viscous layer (1.2 cm), overlying glucose syrup. The resulting deformation pattern is similar to that of experiment 2, although it is more diffuse with a higher fault density, owing to the higher strain rate in this experiment compared to experiment 2. The deformation front continued migrating towards the north until the end of the experiment. Extension continued in the entire deformed region, but the amount of extension absorbed by the region close to the retreating boundary increased.

Figure 9. Experiment 1



A brittle layer was superposed on top of a viscous layer overlying glucose syrup.

Discussion

General discussion

Slab deformation

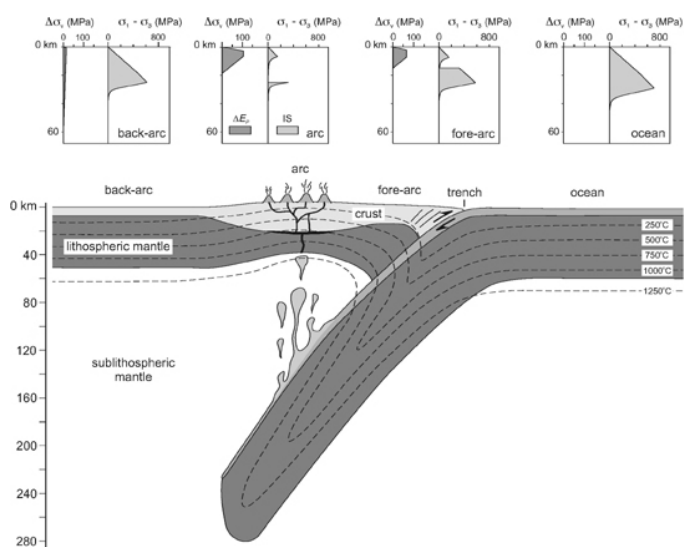
Asymmetrical retreat of a subducting slab requires the least work to deform the slab, simply because it does not involve extensive internal slab deformation. This would be the case in other types of rollback, such as radial rollback. To allow for asymmetrical slab retreat, the only permanent large-scale deformation the subducting plate has to undergo is the formation of a lithospheric-scale vertical tear on one side of the slab segment (Figure 2). Examples of such tears can be observed in several arcs such as the Tonga Arc and the Ryukyu Arc. The formation of a tear could be facilitated by the presence of a pre-existing weak zone in the subducting lithosphere such as a transform fault, striking at high angle to the arc. The presence of a vertical tear at one cusp of the arc would further facilitate asymmetrical rollback, since it would allow lateral asthenosphere flow around the slab in addition to flow underneath the slab tip (Figure 2c). A continuity of the slab across the other cusp would retard rollback of the slab in the proximity of this cusp, since the asthenosphere would only be allowed to flow underneath the slab tip. This process would then amplify the entire process of asymmetrical rollback and back-arc opening. Asymmetrical rollback could also be facilitated by a density polarity in the subducting lithosphere, parallel to the trench axis. This density polarity could result from a variation in age of the subducting slab parallel to the trench or the presence of buoyant features on the subducting plate. With such a slab configuration, the denser part would have a tendency to roll back faster compared to the lighter part, thus promoting asymmetrical rollback.

Overriding plate segmentation

In natural arc systems, slab retreat does not result in the separation between the overriding and subducting plates along the trench. Instead, the overriding plate fails at some distance from the trench. In ocean-ocean subduction settings this often occurs along the volcanic arc, resulting in the formation of a remnant and active volcanic arc, separated by a back-arc basin [Karig 1970, 1971a,b; Kobayashi and Nakada 1979]. Examples include the Tonga-Kermadec Ridge, which was split from the Lau-Colville Ridge during formation of the Lau-Havre Basin. Another example is the Izu-Bonin Arc in the Western Pacific, which was split from

the Palau-Kyushu Ridge during formation of the Parece-Vela Basin. More recently, the active Mariana Ridge was split from the inactive West Mariana Ridge during formation of the Mariana Trough. In ocean-continent subduction settings, back-arc deformation is more diffuse. However, in a more advanced stage of deformation, retreat of the hinge-line can result in the segmentation of the overriding plate, where a segment is being separated from the continent. One example is the Kuril Arc, which separated from the Okhotsk microplate during opening of the Kuril Basin [Maeda 1990]. Another example is the Ryukyu Arc, which is presently being separated from East China, accompanied by extension in the Okinawa Trough [Uyeda 1977]. Other examples include the Japan Arc [Uyeda and Miashiro 1974] and the South Shetland Arc [Lawver 1995].

Figure 6. Schematic sketch of ocean-ocean subduction system

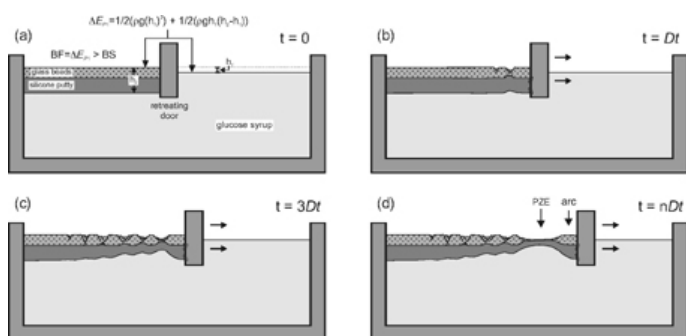


Schematic sketch of ocean-ocean subduction system with inactive back-arc, demonstrating the mechanical weakness and high potential energy (with respect to the subducting lithosphere) of the arc compared to the fore-arc region and the inactive back-arc region, implying that during rollback of the subducting slab, the overriding plate is most likely to break up along the arc. ΔEP = potential energy difference; IS = integrated strength.

A number of arguments can be given for the reason why the overriding plate separates at the arc and not at the trench. First of all, the strength of the overriding plate is at its smallest at the arc due to thermal weakening and its relatively thick crust (Figure 6). Also, the arc has the highest potential energy, further promoting separation along the arc. This excess potential energy results in a net push from

the arc towards the overriding plate, which will therefore not allow separation between the overriding and subducting plate during rollback. Injection of asthenosphere material along the subduction boundary does not occur because of this push from the arc region to the subducting plate, the lithostatic pressure exerted by the overlying mass on the boundary and the net downward drag of material along the subduction boundary due to subduction of the slab.

Figure 7. Schematic sketches illustrating extension observed in experiments

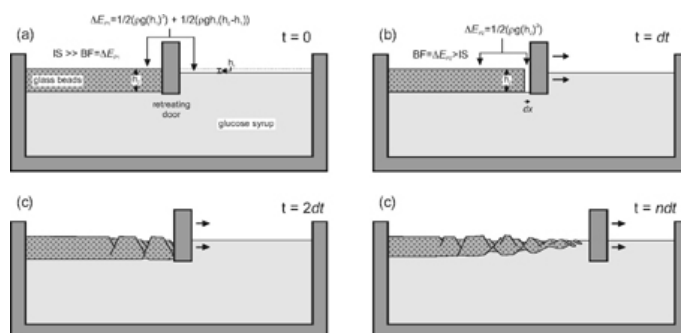


Schematic sketches illustrating extension observed in experiments and the formation of a ridge (i.e. arc) along the retreating door. In most experiments the brittle strength (BS) of a column of lithosphere is smaller than the buoyancy force (BF = potential energy difference (DEP) between column of glass beads and column of glucose syrup). This results in a gradual spreading of the overriding lithosphere during retreat of the door, where the spreading layer remains connected with the retreating door. (a) Initial stage. (b) Initial extension close to the retreating boundary. (c) Continuing retreat leads to a migration of the deformation front. (d) Formation of a principal zone of extension (PZE = zone absorbing most of the extension) and a ridge (arc), which is attached to the retreating door. The location of the PZE and arc could be related to the boudinage of the lithosphere due to retreat of the door, where the silicone layer is not allowed to neck at the contact zone with the door, because this would result in high vertical shear stresses.

In most experiments, no separation between the overriding plate and the retreating door occurred as well, even though the overriding plate was homogeneous throughout. This could be explained by the fact that in most experiments the buoyancy force was greater than the brittle strength of the overriding lithosphere, resulting in spreading of the overriding lithosphere over the glucose syrup in the space it was allowed to by the retreating door (Figure 7). In an advanced stage of deformation, a ridge segment (i.e. arc) developed in between the retreating door and the

principal zone of extension (PZE = a zone which developed in an advanced stage of deformation and subsequently absorbed most or all of the extension during continuing deformation). The location of the PZE and the ridge (arc) could be related to boudinage of the lithosphere due to retreat of the door, where the silicone layer did not favour necking at the contact zone with the door, because this would result in high vertical shear stresses along the contact zone. Thus, it can be concluded that from pure mechanical reasons and even in a homogeneous overriding plate, rollback promotes extension to be localised at some distance from the subduction interface.

Figure 8. Schematic sketches to explain extension



Schematic sketches to explain extension observed in experiment 5 (Figure 4b) and experiment 7 (Figure 4a), where the integrated strength (IS) of a column of glass beads is much greater than the buoyancy force (BF = potential energy difference (DEP)) between column of glass beads and column of glucose syrup). (a) Initial stage. (b) Incremental retreat of the door over a distance dx. DEP between column of glass beads and the gap created by the retreat of the door is greater than the integrated strength of a column of glass beads. (c) Collapse of the glass beads layer towards retreating door. (d) Continued retreat of the door may lead to separation of door from glass beads (e.g. experiment 5).

An interesting question that arises from experiment 5 (and also experiment 5 and 9) is why the overriding plate did not immediately separate from the retreating boundary, but only did so after some considerable deformation of the overriding plate (Figure 4a,b). One would not expect any deformation in the overriding lithosphere due to spreading, since the buoyancy force (between a column of glass beads lithosphere and a column of glucose syrup asthenosphere) in this experiment is a factor of ~ 8-9 smaller (see Table 2) than the integrated strength of the overriding lithosphere. Evidently, the retreating boundary can transmit deviatoric tensional stresses to the overriding lithosphere, without there being any significant adhesion between the glass

beads and the retreating door. An explanation for this behaviour, based on the results of experiment 5, is sketched in Figure 8. From an initial stage (Figure 8a), retreat of the door over a short distance dx leads to the formation of a lithospheric scale gap (Figure 8b), which will not immediately be filled with glucose syrup. This will result in a large potential energy difference between the overriding lithosphere and the gap, leading to the failure and collapse of the overriding lithosphere into the gap (Figure 8c). Extension continues until at some stage the overriding lithosphere separates from the door (Figure 8d).

Discussion (continued)

Natural examples of asymmetrical back-arc extension

Below, we will briefly describe two natural examples of arc - back-arc systems displaying a structural asymmetry. The first example is the Tonga Arc from the southwest Pacific and the second example is the Ryukyu Arc from the Philippine Sea.

Tonga Arc

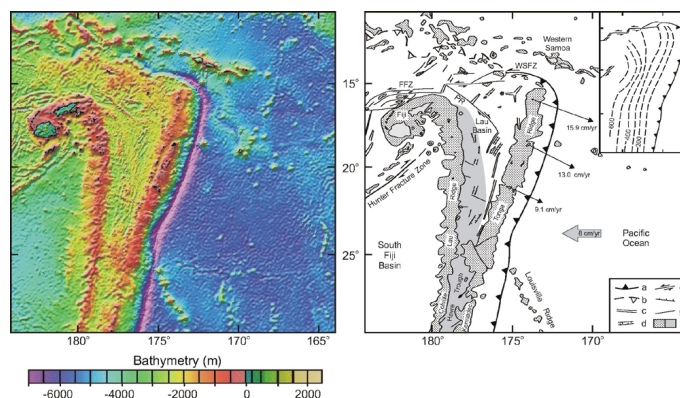
The Tonga-Kermadec Arc system is located in the Southwest Pacific, where the Pacific oceanic lithosphere is subducting westwards along the Tonga-Kermadec Trench underneath the Indo-Australian plate (Figure 9). The Tonga arc is the northernmost half of the Tonga-Kermadec subduction zone, which is usually divided into two arc systems, based on the presence of the Louisville Aseismic Ridge, located on the subducting Pacific plate. From west to east, the overriding plate consists of four distinct zones (Figure 9):

- (1) The South Fiji Basin, an Oligocene back-arc basin floured by oceanic crust [Weissel 1981].
- (2) The Lau-Colville Ridge, which is a remnant volcanic ridge [Karig 1970].
- (3) The Lau-Havre Basin, an active back-arc basin, which started extending at 7-6 Ma [Parson and Hawkins 1994]. Spreading started in the Lau Basin in the north at 5.5-4 Ma and has progressively migrated southward [Parson and Hawkins 1994]. At present the spreading ridge has reached as far as 24° S [Wiedicke and Collier 1993], which is the southern most part of the Lau Basin. The Havre Basin is still in its extensional phase [Gamble and Wright 1995]. The extension is propagating south-southwestward, with

intra-continental extension in the Taupo Volcanic Zone in New Zealand.

- (4) The Tonga-Kermadec Ridge, which is the active volcanic ridge.

Figure 9. Tonga Arc region



(a) Bathymetric map of the Tonga Arc region (from Smith and Sandwell [1997]). (b) Regional tectonic setting of (a) (compiled after Wiedicke and Collier, [1993], Wiedicke and Habler, [1993], Sager *et al.* [1994], Bevis *et al.* [1995], Pelletier *et al.* [1998] and Fujiwara *et al.* [2001]). GPS velocity (thin arrows) of Tonga Arc relative to Australian plate (which includes Fiji block and Lau Ridge) (from Bevis *et al.* [1995]). Thick arrow represents relative convergence between Australian and Pacific plate (from DeMets *et al.* [1994]). Isobaths of Wadati-Benioff zone are shown in inset (100 km contours). a, trench (triangles on upper plate side); b, remnant trench; c, spreading axis; d, graben/trough; e, strike-slip fault; f, normal fault; g, fault (undifferentiated); h, main morphostructural feature on ocean floor (left) and extended crust in back-arc basin (right) (modified from Parson and Hawkins [1994]). FFZ = Fiji Fracture Zone, PR = Peggy Ridge, WSFZ = Western Samoa Fracture Zone. (Click for enlargement)

Two models have been proposed to explain the wedge shaped geometry of the Lau Basin. In the first model the basin supposedly has progressively opened up from north to south (e.g. unzip model [Hawkins 1995]). The second model is the so-called scissors or windscreen wiper model, where the rate of opening of the basin increases northwards [Sager *et al.* 1994; Bevis *et al.* 1995]. A GPS survey of the Tonga Ridge has revealed that the rate of opening increases from south to north and that the Tonga Ridge shows little or no arc parallel deformation [Bevis *et al.* 1995], indicating that the latter model is most applicable. Paleomagnetic data indicates that the Tonga Ridge has rotated ~20° during opening of the Lau Basin, comparable to the amount suggested by the wedge-shaped geometry of the basin itself

[Sager *et al.* 1994]. In the scissors model, the hinge point is defined by the Louisville Seamount chain located at the southern cusp of the arc. At the northern cusp of the arc, deformation is accommodated by the Western Samoa Fracture Zone. Here, the Tonga Arc ends abruptly and the strike of the trench rotates some 90° from north-northeast to west-northwest. At depth, this corresponds to the vertical limit of the Tonga slab at ~ 15°S (Figure 9), which seems to have formed due to tearing between the slab and the Pacific plate at the surface [e.g. Millen and Hamburger 1998]. This tear could have formed due to asymmetric rollback of the Tonga slab, as schematically sketched in Figure 2.

The Lau Basin has formed by two tectonic styles of extension. Initially, the western part of the basin formed by crustal extension and rifting, accompanied by magmatism that partly filled the rift basins [Hawkins 1995]. This was followed by a phase of seafloor spreading [Hawkins 1995] along spreading axes located more to the east. These spreading axes developed on rifts that started from a transform fault boundary [Hawkins 1995].

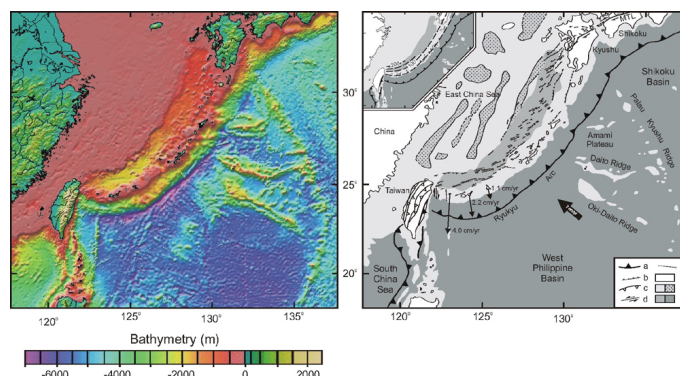
The basin structures can best be compared with the model results presented in Figure 4c, where extension is localised close to the retreating boundary. The model results show that initially extension is absorbed over a wider area, but is later accommodated entirely by a zone located just behind the rifted arc sliver. This is similar to the opening history of the Lau Basin. Furthermore, extensional structures in the basin are mainly parallel to the arc itself, as also observed in the model. This is most probably related to the early stage of opening of the basin. In a later stage of opening, one could expect arc-oblique and perpendicular spreading ridges to form near the hinge point (i.e. near the Louisville Ridge). For instance, this is observed in the North Fiji Basin, which has opened up by ~ 40-50° of rotation of the New Hebrides Arc [Musgrave and Firth 1999]. Here, rift axes and spreading ridges near the northwestern cusp of the arc (i.e. hinge point) are oriented at high angle to the arc but are oriented more parallel to the arc towards the southeast (Figure 1) [Schellart *et al.* 2002a].

Ryukyu Arc

The Ryukyu Arc is located along the South China active margin in an ocean-continent subduction setting. Here, the Philippine Sea plate is subducting northwestward along the Ryukyu Trench underneath the Ryukyu Arc (Figure 10). Two cusps define the lateral extent of the arc. The north-eastern cusp is geographically linked to the Palau-Kyushu

Ridge and the southwestern cusp to Taiwan. The Ryukyu Arc is flanked on the northwestern side by the Okinawa Trough, an active back-arc basin, which has started extending since the Late Miocene [Letouzey and Kimura 1985] and is at present still in a rifting stage. The Ryukyu Arc itself has also experienced deformation from the Late Miocene to Present, with arc parallel as well as arc perpendicular extension [Fournier *et al.* 2001]. The most recent stage of rifting (~ 1 Ma - Present [Miki 1995]) in the Okinawa Trough occurs within a series of en echelon left-stepping grabens trending NE-SW in the north and ENE-WSW in the south (Figure 10) [Sibuet *et al.* 1987]. In the north, the graben axes strike oblique to the main trend of the Okinawa Trough. The crustal thickness beneath the graben axis increases from 15-18 km in the southern part near Taiwan to 27-30 km in the northern part near Kyushu [Iwasaki *et al.* 1990; Sibuet *et al.* 1995].

Figure 10. Bathymetric map of the Ryukyu Arc

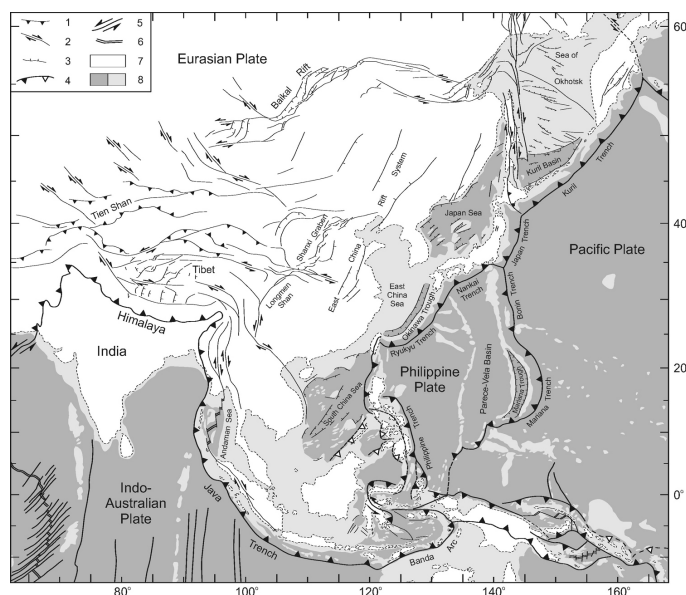


Bathymetric map of the Ryukyu Arc (a) Bathymetric map of the Ryukyu Arc and surrounding (from Smith and Sandwell [1997]). (b) Tectonic interpretation of (a) (compiled after Sibuet *et al.* [1987], Kamata and Kodama [1994] and Lallemand *et al.* [1999]. Horizontal GPS motions of the southern Ryukyu Arc with respect to South China (thin arrows) are from Imanishi *et al.* [1996] and Heki *et al.* [1996]. The relative motion of the Philippine Sea plate with respect to Eurasia (thick arrow) is from Seno *et al.* [1993]. Isobaths (dashed lines) of the Wadati-Benioff zone (for 50, 100, 150 and 200 km) are shown in the inset (from Eguchi and Uyeda [1983]). a, trench (triangles on upper plate); b, normal fault; c, thrust fault; d, strike-slip fault; e, fault (undifferentiated); f, land; g, continental shelf/morphological feature on ocean floor (left) and depression in East China Sea (right) (modified from Hsu *et al.* [2001]); h, Okinawa Trough (left) and continental slope/ocean floor (right). MTL = Median Tectonic Line. (Click for enlargement)

Several models have been proposed to explain the opening of the Okinawa Trough, such as: opening of the Okinawa Trough as a consequence of the collision in Taiwan [Letouzey and Kimura 1985]; opening in a pull-apart fashion due to India-Eurasia collision [Fournier *et al.* 2001]; rollback of the subducting Philippine Sea plate towards the SE [Viallon *et al.* 1986]. We suggest that the extension in the Okinawa Trough is best explained by rollback of the Philippine Sea plate towards the southwest. We propose that the most recent extension is the result of asymmetrical rollback, where the retreat rate increases from northeast to southwest, leading to asymmetrical extension in the overriding plate. Asymmetrical retreat could be explained by the presence of multiple buoyant features located on the subducting lithosphere along the northeastern part of the Ryukyu Trench (e.g. Palau-Kyushu Ridge, Amami Plateau, Daito Ridge, Oki-Daito Ridge). This would imply a higher average lithospheric density along the southwest of the trench compared to the northeast, resulting in a greater rollback velocity in the southwest. Also, a vertical tear in the slab in the southwest of the arc would facilitate the lateral flow of asthenosphere material around the slab edge from underneath the slab towards the slab corner to accommodate rollback (e.g. Figure 2c). This model could explain the en echelon pattern of the individual rift segments in the Okinawa Trough.

The analogue models also show that the obliquity of individual rift systems increases towards the hinge. On a smaller scale, axes of individual rift segments, which are part of large-scale rift systems, are normally oriented oblique to the rift system itself and become progressively more oblique to the rift system towards the hinge. This is also observed for rift segments in the Okinawa Trough. From comparison, experiments 8 and 4 (Figure 4c,e) show most resemblance with the Okinawa Trough. Experiment 4 show the development of a main extensional zone accommodating most of the extension (e.g. Okinawa Trough), located close to the retreating boundary with a narrow strip of material in between (i.e. comparable to the Ryukyu Arc). In the early stages of the experiment extension also occurs along individual rift segments located further away from the retreating boundary, similar to extension observed in the East China Sea (Figure 10). The extension in the north stopped after a through-going rift zone developed in experiment 4, similar to the extension in the East China Sea, which stopped after initiation of formation of the Okinawa Trough [Hsu *et al.* 2001].

Figure 11. Comparison between analogue results and structures



Comparison between analogue results of experiment 8 and structures in the overriding plate around the Palau-kyushu Ridge (from Smith and Sandwell [1997]). (a) Bathymetric map surrounding the northeastern cusp of the Ryukyu Arc. (b) Tectonic interpretation of (a) (compiled after Sibuet *et al.* [1987] and Kamata and Kodama [1994]. Paleomagnetic declinations from Kodama and Nakayama [1993] and Kodama *et al.* [1995]. (c) Results of experiment after 30° rotation. (d) Interpretation of (c). a, trench (triangles on upper plate); b, normal fault; c, thrust fault; d, strike-slip fault; e, fault (undifferentiated); f, land; g, continental shelf/morphological feature on ocean floor (left) and depression in East China Sea (right) (modified from Hsu *et al.* [2001]); h, Okinawa Trough (left) and continental slope/ocean floor (right). MTL = Median Tectonic Line; OKTL = Oita-Kumamoto Tectonic Line. (Click for enlargement)

Another interesting analogy between model and nature is the presence of the Oita-Kumamoto Tectonic Line (Figure 11a,b), a dextral strike-slip fault, which could be compared with the occurrence of dextral strike-slip faults near the hinge in most of the analogue experiments with a similar orientation compared to the trench (Figure 11c,d). In most tectonic interpretations the Median Tectonic Line, located to the east of the Oita-Kumamoto Tectonic Line, has been interpreted as resulting from strain partitioning in the overriding plate due to oblique subduction of the Philippine Sea plate [Tsukuda 1992; Kamata and Kodama 1994]. This interpretation could correct for the Median Tectonic Line *sensu stricto*. However, in the light of the experiments presented here, its westernmost extension

outcropping on Kyushu Island (Oita-Kumamoto Tectonic Line) could also be a mere effect of rotation of the arc segment located close to the hinge point. Interestingly enough, Kamata and Kodama [1994] have noted the synchronous occurrence of dextral shearing along the Oita-Kumamoto Tectonic Line, anticlockwise rotation of the northeastern Ryukyu Arc and the formation of rift segments striking oblique to the tectonic lineament.

The Wadati-Benioff zone of the subducting Philippine slab increases in depth from the northeast to the southwest, where it abruptly ends in the southwest just east of Taiwan (Figure 10). This could imply a greater slab length (or at least a colder slab) in the southwest and therefore a greater slab pull force, resulting in faster rollback in the southwest. This increase in retreat is facilitated in the southwest by the discontinuity of the slab, which allows asthenosphere material to flow underneath the slab tip from the ocean side towards the asthenosphere wedge, as well as horizontally around the slab edge. This is not possible in the northeast due to the continuity of the slab across the northeastern cusp. The increase in retreat velocity along the subduction zone is supported by recent GPS data from the southern Ryukyu Arc (Figure 10) [Imanishi *et al.* 1996; Heki *et al.* 1996] and could explain the southwestward decrease in crustal thickness of the Okinawa Trough. The abrupt ending of the slab in the southwest seems to represent a vertical tear, where the horizontal projection of this tear is oriented north-south and closely coincides with the steep continental margin of eastern Taiwan, also striking north-south. This leads to the tentative conclusion that whilst the Philippine slab is retreating towards the south to southwest, it is forming a tear between the buoyant (continental) part of the Philippine plate (Taiwan) and the dense (oceanic) part of the Philippine plate. The location of this tear could be triggered by the transition from continental to oceanic lithosphere.

Other examples

Another example of asymmetrical arc systems is the New Hebrides Arc from the southwest Pacific (Schellart *et al.* 2002a). This arc system is situated in an ocean-ocean subduction setting and is flanked by the North Fiji Basin, a wedge-shaped active back-arc basin, which developed since ~ 12-11 Ma [Pelletier *et al.* 1993] due to asymmetrical clockwise opening (Figure 1). In an initial stage of opening, back-arc spreading ridges had a strike ~ parallel to the arc (Figure 1b), but in a later stage this pattern became more

complicated with arc-oblique spreading ridges near the hinge point (Figure 1c). The most recent stage of development of the arc and back-arc basin has been complicated by subduction of the d'Entrecasteaux Ridge and the West Torres Plateau.

The Kuril Arc system could also be regarded as a system that has developed to a large extent by asymmetrical rollback. The system is situated in an ocean-continent subduction setting and is flanked by the Kuril Basin and the Sea of Okhotsk, which developed by anticlockwise retreat of the Pacific slab from the Eocene until the Middle Miocene. The back-arc region is characterised by diffuse deformation in the Sea of Okhotsk and a late stage opening of the Kuril Basin, which is thought to be underlain by oceanic crust.

The New Hebrides Arc system and the Kuril Arc system will be discussed more extensively elsewhere [Schellart *et al.*, in press; Schellart *et al.*, submitted].

Conclusions

Several back-arc basins display a geometry and internal structure that is asymmetric, i.e. where the amount of extension increases from one end of the arc to the other. We presented a simple model to explain this geometry, where the opening is controlled by rollback of the hinge-line of the subducting lithosphere. The increase in extension is explained by the increase in retreat velocity of the subducting slab along the trench axis. This increase in velocity can be caused by an increase in lithospheric density along the trench axis and/or a vertical tear in the slab at the more rapidly retreating side of the retreating slab. We have presented the results of 3-dimensional analogue models to simulate asymmetrical back-arc extension of an overriding lithosphere. In these models the initial rheology has been varied. The results show that with increasing lithospheric brittle to viscous strength (BS/VS), the fault density decreases, while the asymmetry in deformation pattern in the back-arc region increases. It is also shown that with decreasing brittle strength to buoyancy force ratio (BS/BF) the total area of surface deformation increases. The models and experimental results can be compared with several arc - back-arc systems, which display a relatively large amount of asymmetry along the arc and in the back-arc region (e.g. Tonga Arc, Kuril Arc, New Hebrides Arc, Ryukyu arc) but a varying style of tectonic deformation. These differences

are mainly the result of the stage of opening up of the back-arc basin and differences in rheology of the overriding lithosphere.

The analogue results indicate that with an initially buoyant and weak overriding plate rheology, deformation can propagate inboard far from the retreating boundary, where the amount of propagation is comparable to the width of the retreating boundary. We make the tentative proposition that extension and strike-slip faulting observed in East Asia do not necessarily have to be related to escape tectonics due to India-Eurasia collision. These structures could also be

explained by tensional deviatoric stresses along the East Asian active margin due to slab retreat towards the east-southeast. During the Oligocene to Middle Miocene, back-arc extension along the East Asian margin took place along a continuous zone of more than 6000 km in length, stretching from the South China Sea in the southwest to the Sea of Okhotsk in the northeast. This could have led to extension in the overriding plate at a distance as far as 3000-4000 km away from the active margin, such as extension in the Shanxi graben and the Baikal rift.

References

- Auzende, J.-M., Y. Lafoy, and B. Marsset, Recent geodynamic evolution of the North Fiji Basin (Southwest Pacific), *Geology*, 16, 925-929, 1988.
- Beck, R.A., D.W. Burbank, W.J. Sercombe, G.W. Riley, J.K. Barndt, J.R. Berry, J. Afzal, A.M. Khan, H. Jurgens, J. Metje, A. Cheema, N.A. Shafique, R.D. Lawrence, and M.A. Khan, Stratigraphic evidence for an early collision between Northwest India and Asia, *Nature*, 373, 55-58, 1995.
- Bevis, M., F.W. Taylor, B.E. Schutz, J. Recy, B.L. Isacks, S. Helu, R. Singh, E. Kendrick, J. Stowell, B. Taylor, and S. Calmant, Geodetic observations of very rapid convergence and back-arc extension at the Tonga Arc, *Nature*, 374, 249-251, 1995.
- Cobbold, P.R., and M.P.A. Jackson, Gum rosin (colophony); a suitable material for thermomechanical modelling of the lithosphere, *Tectonophysics*, 210, 255-271, 1992.
- Coulomb, C.A., Sur une application des règles maximis et minimis a quelques problèmes de statique, relatifs à l'architecture, *Mémoires de Mathématique et de Physique, Académie Royale des Sciences*, 7, 343-382, 1776.
- Curry, J.R., D.G. Moore, L.A. Lawver, F.J. Emmel, R.W. Raitt, M. Henry, and R. Kieckhefer, Tectonics of the Andaman Sea and Burma, in *Geological and geophysical investigations of continental margins*. AAPG Memoir, edited by J.S. Watkins, L. Montadert, and P.W. Dickerson, pp. 189-198, 1979.
- Davy, P., and P.R. Cobbold, Indentation tectonics in nature and experiment. 1. Experiments scaled for gravity, *Bulletin of the Geological Institutions of the University of Uppsala, N.S.*, 14, 129-141, 1988.
- Davy, P., and P.R. Cobbold, Experiments on shortening of a 4-layer model of the continental lithosphere, *Tectonophysics*, 188, 1-25, 1991.
- DeMets, C., R.G. Gordon, D.F. Argus, and S. Stein, Effect of recent revisions to the geomagnetic reversal time scale on estimates of current plate motions, *Geophysical Research Letters*, 21, 2191-2194, 1994.
- Eguchi, T., and S. Uyeda, Seismotectonics of the Okinawa Trough and Ryukyu Arc, in *Chung Kuo Ti Ch'ih Hsueh Hui Chuan Kan = Memoir of the Geological Society of China*, pp. 189-210, 1983.
- Elsasser, W.M., Sea-floor spreading as thermal convection, *Journal of Geophysical Research*, 76, 1101-1112, 1971.
- England, P.C., G.A. Houseman, The mechanics of the Tibetan Plateau, *Philosophical Transactions of the Royal Society of London, Series A: Mathematical and Physical Sciences*, 326, 301-320, 1988.
- Fournier, M., O. Fabbri, J. Angelier, and J.-P. Cadet, Regional Seismicity and on-land deformation in the Ryukyu arc: Implications for the kinematics of opening of the Okinawa Trough, *Journal of Geophysical Research*, 106, 13751-13768, 2001.
- Fujiwara, T., T. Yamazaki, and M. Joshima, Bathymetry and magnetic anomalies in the Havre Trough and southern Lau Basin; from rifting to spreading in back-arc basins, *Earth and Planetary Science Letters*, 185, 253-264, 2001.
- Gamble, J.A., and I.C. Wright, The Southern Havre Trough geological structure and magma petrogenesis of an active backarc rift complex, in *Backarc basins: tectonics and magmatism*, edited by B. Taylor, pp. 29-62, Plenum Press, New York, 1995.
- Gautier, P., J.-P. Brun, R. Moriceau, D. Sokoutis, J. Martinod, and L. Jolivet, Timing, kinematics and cause of Aegean extension; a scenario based on a comparison with simple analogue experiments, *Tectonophysics*, 315, 31-72, 1999.
- Hathway, B., The Nadi Basin; Neogene strike-slip faulting and sedimentation in a fragmented arc, western Viti Levu, Fiji, *Journal of the Geological Society of London*, 150, 563-581, 1993.
- Hatzfeld, D., J. Martinod, G. Bastet, and P. Gautier, An analog experiment for the Aegean to describe the contribution of gravitational potential energy, *Journal of Geophysical Research*, 102, 649-659, 1997.
- Hawkins, J.W., The geology of the Lau Basin, in *Backarc basins: tectonics and magmatism*, edited by B. Taylor, pp. 63-138, Plenum Press, New York, 1995.
- Heki, K., Horizontal and vertical crustal movements from three-dimensional very long baseline interferometry kinematic reference frame; implication for the reversal timescale revision, *Journal of Geophysical Research*, 101, 3187-3198, 1996.
- Horsfield, W.T., An experimental approach to basement-controlled faulting, *Geologie en Mijnbouw*, 56, 363-370, 1977.
- Hsu, S.-K., J.C. Sibuet, and C.T. Shyu, Magnetic inversion in the East China Sea and Okinawa Trough: tectonic implications, *Tectonophysics*, 333, 111-122, 2001.
- Hubbert, M.K., Theory of scale models as applied to the study of geologic structures, *Geological Society of America Bulletin*, 48, 1459-1520, 1937.
- Imanishi, M., F. Kimata, N. Inamori, R. Miyajima, T. Okuda, K. Takai, K. Hirahara, and T. Kato, Horizontal displacements by GPS measurements at the Okinawa-Sakishima Islands (1994-1995), *Zisin = Jishin*, 49, 417-421, 1996.
- Iwasaki, T., N. Hirata, T. Kanazawa, J. Melles, K. Suyehiro, T. Urabe, L. Moeller, J. Makris, and H. Shimamura, Crustal and upper mantle structure in the Ryukyu Island Arc deduced from deep seismic sounding, *Geophysical Journal International*, 102, 631-657, 1990.
- Jolivet, L., K. Tamaki, and M. Fournier, Japan Sea, opening history and mechanism; a synthesis, *Journal of Geophysical Research*, 99, 22,237-22,259, 1994.

- Kamata, H., and K. Kodama, Tectonics of an arc-arc junction; an example from Kyushu Island at the junction of the Southwest Japan Arc and the Ryukyu Arc, *Tectonophysics*, 233, 69-81, 1994.
- Karig, D.E., Ridges and basins of the Tonga-Kermadec island arc system, *Journal of Geophysical Research*, 75, 239-254, 1970.
- Karig, D.E., Origin and development of marginal basins in the western Pacific, *Journal of Geophysical Research*, 76, 2542-2561, 1971.
- Karig, D.E., Structural history of the Mariana island arc system, *Geological Society of America Bulletin*, 82, 323-344, 1971.
- Kobayashi, K., and M. Nakada, Magnetic anomalies and tectonic evolution of the Shikoku inter-arc basin, in *Geodynamics of the Western Pacific*, edited by S. Uyeda, R. Murphy, and K. Kobayashi, pp. 391-402, Jpn. Sci. Soc. Press, Tokyo, 1979.
- Kodama, K., and K.-i. Nakayama, Paleomagnetic evidence for post-late Miocene intra-arc rotation of South Kyushu, Japan, *Tectonics*, 12, 35-48, 1993.
- Kodama, K., H. Tashiro, and T. Takeuchi, Quaternary counterclockwise rotation of South Kyushu, Southwest Japan, *Geology*, 23, 823-826, 1995.
- Lallemant, S., C.-S. Liu, S. Dominguez, P. Schnuerle, and J. Malavieille, Trench-parallel stretching and folding of forearc basins and lateral migration of the accretionary wedge in the southern Ryukyus; a case of strain partition caused by oblique convergence, *Tectonics*, 18, 231-247, 1999.
- Lawver, L.A., R.A. Keller, M.R. Fisk, and J.A. Strelin, Bransfield strait, Antarctic Peninsula: active extension behind a dead arc, in *Backarc basins: tectonics and magmatism*, edited by B. Taylor, pp. 315-342, Plenum Press, New York, 1995.
- Letouzey, J., and M. Kimura, Okinawa Trough genesis; structure and evolution of a backarc basin developed in a continent, *Marine and Petroleum Geology*, 2, 111-130, 1985.
- Maeda, J.i., Opening of the Kuril Basin deduced from the magmatic history of central Hokkaido, North Japan, *Tectonophysics*, 174, 235-255, 1990.
- Malahoff, A., R.H. Feden, and H.S. Fleming, Magnetic anomalies and tectonic fabric of marginal basins north of New Zealand, *Journal of Geophysical Research*, 87, 4109-4125, 1982.
- Martinod, J., D. Hatzfeld, J.P. Brun, P. Davy, and P. Gautier, Continental collision, gravity spreading, and kinematics of Aegea and Anatolia, *Tectonics*, 19, 290-299, 2000.
- Miki, M., Two-phase opening model for the Okinawa Trough inferred from paleomagnetic study of the Ryukyu Arc, *Journal of Geophysical Research*, 100, 8169-8184, 1995.
- Millen, D.W., and M.W. Hamburger, Seismological evidence for tearing of the Pacific Plate at the northern termination of the Tonga subduction zone, *Geology*, 26, 659-662, 1998.
- Molnar, P., and T. Atwater, Interarc spreading and Cordilleran tectonics as alternates related to the age of subducted oceanic lithosphere, *Earth and Planetary Science Letters*, 41, 330-340, 1978.
- Molnar, P., and P. Tapponnier, Cenozoic tectonics of Asia: effects of a continental collision, *Science*, 189, 419-426, 1975.
- Molnar, P., and P. Tapponnier, Relation of the tectonics of eastern China to the India-Eurasia collision; application of slip-line field theory to large-scale continental tectonics, *Geology*, 5, 212-216, 1977.
- Musgrave, R.J., and J.V. Firth, Magnitude and timing of New Hebrides Arc rotation; paleomagnetic evidence from Nendo, Solomon Islands, *Journal of Geophysical Research*, 104, 2841-2853, 1999.
- Northrup, C.J., L.H. Royden, and B.C. Burchfiel, Motion of the Pacific Plate relative to Eurasia and its potential relation to Cenozoic extension along the eastern margin of Eurasia, *Geology*, 23, 719-722, 1995.
- Parson, L.M., and J.W. Hawkins, Two-stage ridge propagation and the geological history of the Lau backarc Basin, *Proceedings of the Ocean Drilling Program, Scientific Results*, 135, 819-828, 1994.
- Pelletier, B., S. Calmant, and R. Pillet, Current tectonics of the Tonga-New Hebrides region, *Earth and Planetary Science Letters*, 164, 263-276, 1998.
- Pelletier, B., Y. Lafoy, and F. Missegue, Morphostructure and magnetic fabric of the northwestern North Fiji Basin, *Geophysical Research Letters*, 20, 1151-1154, 1993.
- Peltzer, G., Centrifuged experiments of continental scale tectonics in Asia, *Bulletin of the Geological Institutions of the University of Uppsala, N.S.*, 14, 115-128, 1988.
- Polachan, S., and A. Racey, Stratigraphy of the Mergui Basin, Andaman Sea; implications for petroleum exploration, *Journal of Petroleum Geology*, 17, 373-406, 1994.
- Ratschbacher, L., O. Merle, P. Davy, and P. Cobbold, Lateral extrusion in the Eastern Alps: Part 1, Boundary conditions and experiments scaled for gravity, *Tectonics*, 10, 245-256, 1991.
- Sager, W.W., C.J. Macleod, and N. Abrahamsen, Paleomagnetic constraints on Tonga Arc tectonic rotation from sediments drilled at sites 840 and 841, *Proceedings of the Ocean Drilling Program, Scientific Results*, 135, 763-783, 1994.
- Schellart, W.P., Shear test results for cohesion and friction coefficients for different granular materials: scaling implications for their usage in analogue modelling, *Tectonophysics*, 324, 1-16, 2000.
- Schellart, W.P., M.W. Jessell, and G.S. Lister, Asymmetrical extension in the back-arc region of the Kuril Arc, Northwest Pacific: Some insights from analogue modeling, submitted.

- Schellart, W.P., G.S. Lister, and M.W. Jessell, Analogue modeling of arc and backarc deformation in the New Hebrides arc and North Fiji Basin, *Geology*, 30, 311-314, 2002a.
- Schellart, W.P., G.S. Lister, and M.W. Jessell, Some experimental insights into arc formation and back-arc extension, *Bollettino di Geofisica Teorica ed Applicata*, 42 (suppl. 1/2), 85-91, 2002b.
- Searle, M.P., B.F. Windley, M.P. Coward, D.J.W. Cooper, A.J. Rex, D. Rex, L. Tingdong, X. Xuchang, M.Q. Jan, V.C. Thakur, and S. Kumar, The closing of Tethys and the tectonics of the Himalaya, *Geological Society of America Bulletin*, 98, 678-701, 1987.
- Seno, T., S. Stein, and A.E. Gripp, A model for the motion of the Philippine Sea Plate consistent with NUVEL-1 and geological data, *Journal of Geophysical Research*, 98, 17941-17948, 1993.
- Sibuet, J.-C., J. Letouzey, F. Barbier, J. Charvet, J.-P. Foucher, T.W.C. Hilde, M. Kimura, C. Ling-Yun, B. Marsset, C. Muller, and J.-F.
- Stephan, Back arc extension in the Okinawa Trough, *Journal of Geophysical Research*, 92, 14041-14063, 1987.
- Sibuet, J.C., S.-K. Hsu, C.T. Shyu, and C.S. Liu, Structural and kinematic evolution of the Okinawa Trough backarc basin, in *Backarc basins: tectonics and magmatism*, edited by B. Taylor, pp. 343-379, Plenum Press, New York, 1995.
- Smith, W.H.F., and D.T. Sandwell, Global sea floor topography from satellite altimetry and ship depth soundings, *Science*, 277, 1956-1962, 1997.
- Tapponnier, R., G. Peltzer, A.Y. Le Dain, R. Armijo, and P. Cobbold, Propagating extrusion tectonics in Asia; new insights from simple experiments with plasticine, *Geology*, 10, 611-616, 1982.
- Uyeda, S., Some basic problems in the trench-arc-back arc system, in *Island arcs, deep sea trenches and back-arc basins*, Maurice Ewing Series, edited by M. Talwani, and W.C. Pitman, pp. 1-14, Harriman, New York, 1977.
- Uyeda, S., and A. Miyashiro, Plate Tectonics and the Japanese Island; A Synthesis, *Geological Society of America Bulletin*, 85, 1159-1170, 1974.
- Viallon, C., P. Huchon, and E. Barrier, Opening of the Okinawa Basin and collision in Taiwan: a retreating trench model with lateral anchoring, *Earth and Planetary Science Letters*, 80, 145-155, 1986.
- Weissel, J.K., Magnetic lineations in marginal basins of the western Pacific, *Philosophical Transactions of the Royal Society of London, Series A: Mathematical and Physical Sciences*, 300, 223-247, 1981.
- Wiedicke, M., and J. Collier, Morphology of the Valu Fa spreading ridge in the southern Lau Basin, *Journal of Geophysical Research*, 98, 11769-11782, 1993.
- Worrall, D.M., V. Kruglyak, F. Kunst, and V. Kuznetsov, Tertiary tectonics of the Sea of Okhotsk, Russia: Far-field effects of the India-Eurasia collision, *Tectonics*, 15, 813-826, 1996.
- Yin, A., Mode of Cenozoic east-west extension in Tibet suggesting a common origin of rifts in Asia during the Indo-Asia Collision, *Journal of Geophysical Research*, 105, 21745-21759, 2000.
- Yu, H.-S., The Pearl River Mouth Basin: A rift basin and its geodynamic relationship with the southeastern Eurasian margin, *Tectonophysics*, 183, 177-186, 1990.
- Zhou, D., K. Ru, and H. Chen, Kinematics of Cenozoic extension on the South China Sea continental margin and its implications for the tectonic evolution of the region, *Tectonophysics*, 251, 161-177, 1995.